geoconvention
Calgary • Canada • June 20-22 2022

Time-lapse VSP detection of a simulated shallow CO_2 leak at the CaMI Field Research Station

Brendan J. Kolkman-Quinn, Donald C. Lawton
CREWES, University of Calgary, Containment and Monitoring Institute

Summary

Effective geophysical monitoring is essential for Measurement, Monitoring and Verification (MMV) of geological CO_2 sequestration. The Containment and Monitoring Institute Field Research Station (CaMI.FRS) near Brooks, Alberta was developed to test monitoring technologies and inform MMV expectations for larger scale operations. CO_2 is currently being injected at 300m depth into the Basal Belly River Sandstone, a brine aquifer of 10% porosity at the base of the Foremost Fm (Dongas, 2016, Macquet and Lawton, 2017). Various geophysical and geochemical monitoring technologies are tested at the FRS, including time-lapse vertical seismic profiles (VSP). Results from CaMI.FRS provide unique field data relevant to shallow-leak detection from Carbon Capture and Storage (CCS) and Enhanced Oil Recovery (EOR) operations in sedimentary basins. VSP data were collected between 2017 and 2021 using geophones and Distributed Acoustic Sensing (DAS). Monitor surveys provided snapshots of the reservoir with cumulative CO_2 injection amounts of 7 t, 15 t, and 33 t of CO_2. These field data had high repeatability, with permanent sensors in an observation well and nearly-identical shot coordinates. Variable weather-related filtering effects at the surface and near-surface were the main source of dissimilarity between baseline and monitor surveys. The 10Hz-150Hz field data required cautious processing and the development of a reliable, time-lapse compliant workflow. This produced directly comparable amplitudes between baseline and monitor surveys without the need for cross-equalization using shaping filters. The CO_2 plume was confidently detected and delineated on borehole geophone data after 33 t of injection, but not yet on equivalent DAS time-lapse data. The DAS baseline and monitoring data were collected with different interrogators and also showed different noise levels. Compared to the high SNR geophone data, the DAS data required additional data-preparation steps and aggressive de-noising. Only one monitoring line, with the least noisy baseline data, showed a weak CO_2 time-lapse anomaly similar to the geophone results. Surpassing the detection threshold between 15 t and 33 t of injected CO_2 appears to represent the limit of detectability for a shallow CO2 leak in the particular geological setting at the CaMI.FRS. The 33 t detection threshold and the time-lapse compliant workflow provide insight into the challenges and capabilities of shallow leak detection, and of monitoring shallow CO_2 sequestration.

Workflow

The time-lapse compliant VSP processing workflow was developed by streamlining and simplifying standard VSP workflows previous employed at the FRS by Kolkman-Quinn and Lawton (2020) and Gordon (2019). These were originally based on Hinds and Kuzmiski (1996) and the recommended workflows from Schulmberger's VISTA processing software. A detailed explanation of the time-lapse compliant workflow is given by Kolkman-Quinn (2022). Numerous

processing steps were deemed unnecessary and were eliminated as possible sources of major and minor error, which had caused dissimilarity between baseline and monitor data. Crucially, trace-normalization by first arrival amplitude was removed. This had previously been done with a mean scaling operation based off direct arrival amplitudes. This was found to be redundant and error prone. The deterministic deconvolution possible with VSP data achieves trace-normalization directly and at all frequencies in a single step. This produced directly comparable amplitudes at all frequencies with minimal error, save for the highest frequency bands where variable weather-related near-surface filtering could not be reversed by the deconvolution. 3-component data rotation and wavefield separation was removed due to an increasing number of dead traces in the horizontal components, requiring interpolation and risking the introduction of unnecessary error. Processing was performed using only the vertical components of the geophones, in this iteration of the workflow. This 1-C workflow was directly applicable to straight-fiber DAS data. With successful results from the 1-C workflow, re-introducing the 3-C data can now be attempted. Wavefield separation was achieved with a median filter and f-k filter rather than time-variant 3-C rotation, similar to zero-offset data. This was mainly possible due to the 250 m shot offset range not causing significant NMO errors for the 300 m deep reservoir, nor requiring pre-stack migration for the relatively flat layering. Time-variant data rotation and migration will be tested as farther offset shots are incorporated into the monitoring program with the growth of the CO_2 plume. In addition to the trace-normalization and 3-C processing steps, unnecessary filtering steps such as median and f-k filters on the processed, pre-stack data were removed from the VSP CDP stacking process. These were minor sources of error but were found to be unnecessary. Figure 1 shows a flow-chart of the simplified, time-lapse compliant processing workflow.

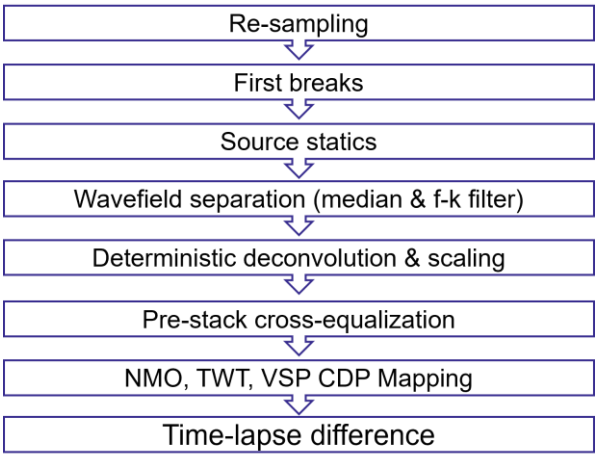

Figure 1. This simplified VSP processing workflow produced highly reliable time-lapse results with the CaMI.FRS data. The workflow is described in detail by Kolkman-Quinn (2022).

The third major source of error eliminated for this workflow was the use of shaping filters, and RMS trace amplitude normalization for cross-equalization. The use of shaping filters had originally based on work by Cheng et al. (2010) from the Frio CO_2 injection project and was considered standard for time-lapse seismic cross-equalization. Shaping filters designed from both the downgoing direct arrivals and the upgoing reflected arrivals were attempted with the CaMI.FRS

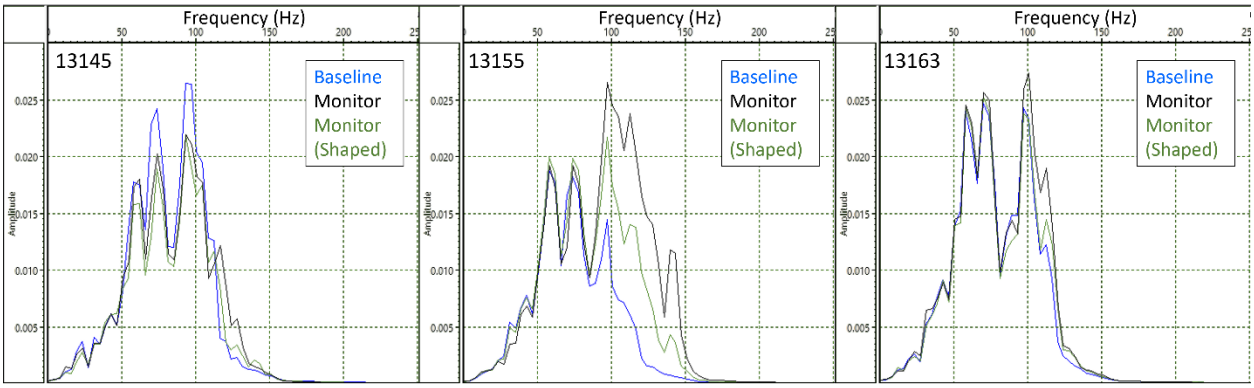

Figure 2 Three examples of shot gather spectra from baseline (blue) and monitor (black) processed shot gathers. Deconvolution alone correctly scaled the amplitudes at each frequency up to a point of divergence where weather-related near-surface filtering was not fully reversed. Minor disparities in frequency content were addressed by shaping filters (green) but not major ones, such as in shot 13155.

datasets. The higher frequencies had suffered from variable weather-related near-surface filtering in the baseline and monitor data and these effects were only partially reversed during deconvolution. The upgoing-designed shaping filter was found to needlessly influence the BBRS reflection and diminish the time-lapse anomaly, while inadequately matching the highest frequency bands. This produced high-frequency residuals from the most mis-matched shot gathers. The downgoing-designed shaping filter was designed independent of the reflection data and did not unduly affect the reflection amplitudes. However, it was insensitive to the low-amplitude, highly attenuated higher frequency bands and failed to address the near-surface filtering problem. These spectrum disparities again produced high-frequency residuals (Figure 2).

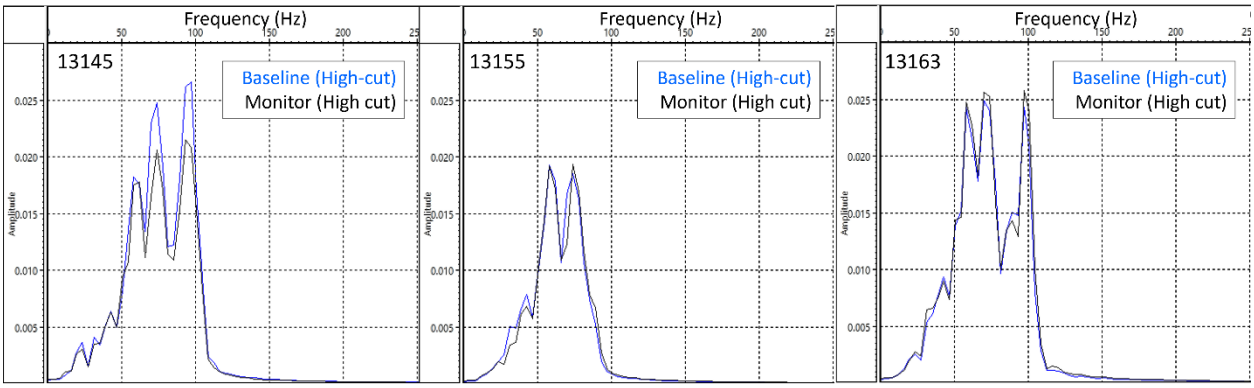

Figure 3. High-cut filtering after deconvolution trimmed the baseline and monitor spectra to a common bandwidth. Shot 13145 reflected off the CO_2 plume and the corresponding amplitude reduction is visible in the monitor spectrum (black) compared to the baseline (blue).

Rather than use a shaping filter, shot-specific high-cut filters were developed to simply remove the lingering effects of weather-related near-surface filtering from the otherwise directly comparable baseline and monitor data. This required a laborious shot-by-shot inspection of amplitude spectra, in a manual process that could be automated for larger datasets. The high-cut

filtered spectra can be seen in Figure 3. With the unresolved weather-related near-surface filtering removed from the spectra, the baseline amplitudes could be directly subtracted from the monitor data without need of further cross-equalization. Shot 13145 in Figure 3 reflected off the CO_2 plume, and shows the preserved amplitude difference caused by CO_2 saturation. This causes a reflection amplitude anomaly in the difference between VSP CDP stacked baseline and monitor data.

Results and Conclusions

The CO_2 anomaly manifests as a trough-peak succession with side-lobe energy, caused by a reduction in impedance in the BBRS reservoir. CO_2 saturation in the BBRS reservoir causes a decrease in P-wave velocity, with minimal effect on S-wave velocity and density (Macquet et al., 2019). This produces a trough-peak seismic anomaly with side-lobe energy at the top and bottom of the BBRS reservoir. Under the reflection anomaly, a weaker anomaly is caused by travel-time delay through the reservoir in the monitor survey. A finite difference VSP forward model set expectations of the plume's signature and extent (Figure 4). This model did not include random noise as it was mainly used for setting expectations and testing elements of the processing workflow.

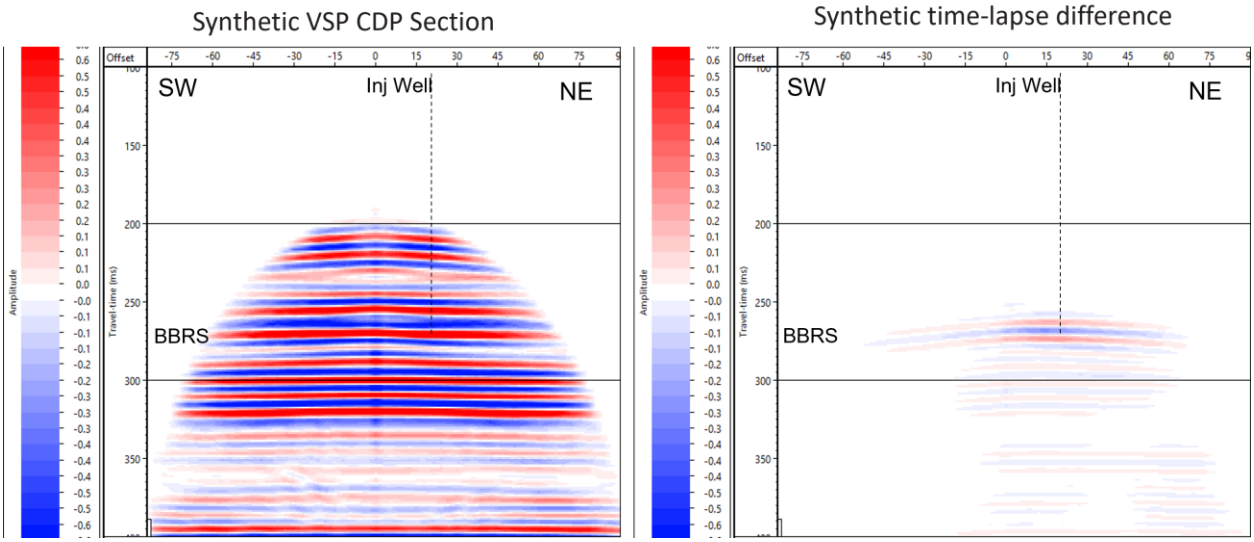

Figure 4. Forward model of the CO_2 anomaly in the BBRS interval, from a finite difference VSP model. The anomaly is a trough-peak succession with side-lobe energy, followed by a weaker anomaly caused by travel-time delay in the monitor data.

Due to the relatively low porosity of up to 10% in this injection interval, the partial saturation of brine with CO_2 produces a modest decrease in P-wave velocity, rather than a precipitous drop more typical of high porosity (e.g. 25%-30%) reservoirs (Figure 5). Fluid substitution modeling by Macquet et al. (2019) set expectations for a subtle amplitude anomaly in the time-lapse seismic data, motivating the development of a reliable time-lapse compliant workflow with few sources of error.

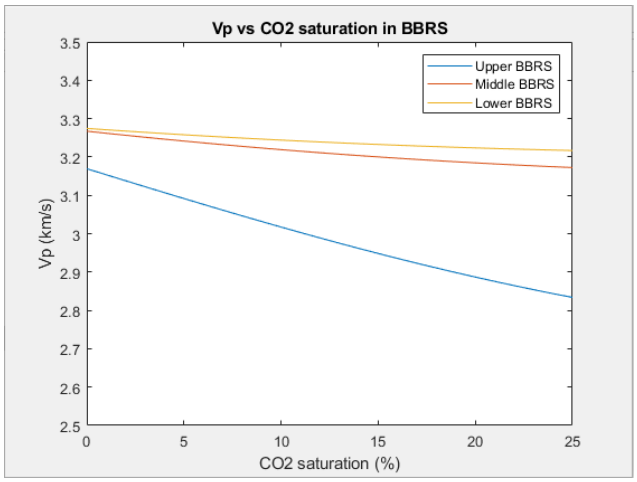

Figure 5. The relatively low porosity of the injection interval causes partial CO_2 saturation to produce gradual P-wave reductions. This produces a subtle amplitude anomaly in the time-lapse difference, motivating the development of a reliable time-lapse compliant processing workflow. P-wave velocities are reduced by 1%-10% depending on the geology within the reservoir, with CO_2 saturation of 25%.

After pre-stack high-cut filtering each baseline and monitor shot gather pair, the baseline was directly subtracted from the monitor data to produce a time-lapse difference. Figure 6 shows examples of the time-lapse results from two of the three principle monitoring lines at CaMI.FRS. Panels a and b show 1 year and 2 year time-lapse corresponding to 7 t and 15 t of injected CO_2.

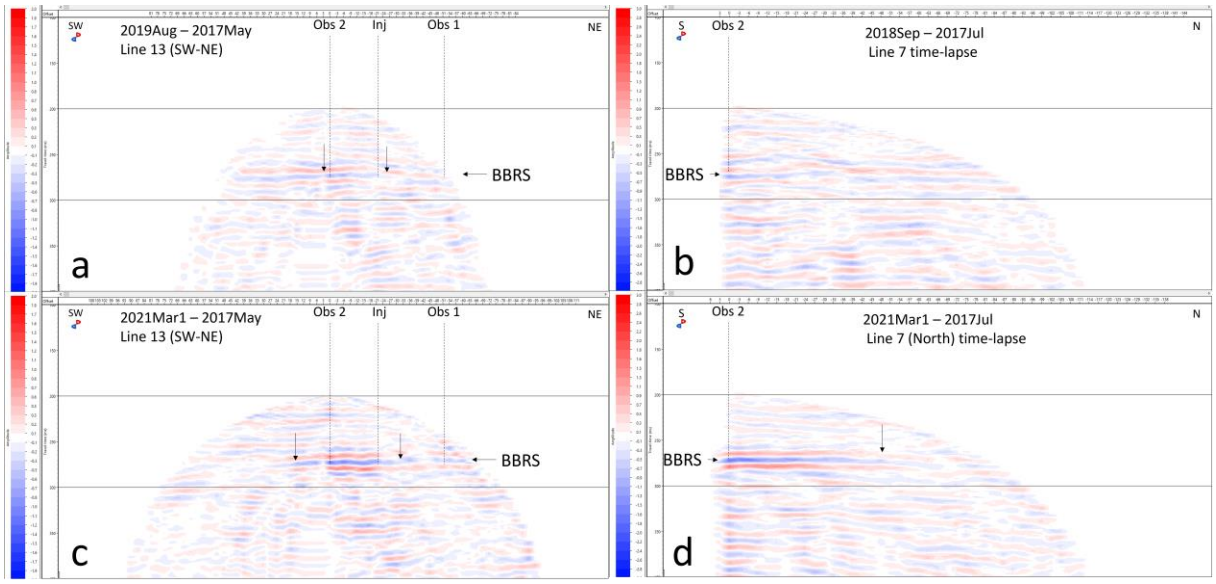

Figure 3. Time-lapse differences of VSP CDP stacked data from CaMI.FRS. The 2019 monitoring survey did not unequivocally detect the 15 t CO_2 plume around the Injection well (a), while the plume had not extended to the north monitoring line (b). Unambiguous amplitude anomalies caused by CO_2 are evident by March, 2021 (c & d).

Figure 6b & 6d show only half of a full walk-away VSP CDP survey, as only the northern half of that line was available in that particular survey. The south side will be available for future results. In addition, the 2019 monitor survey for Figure 6a had a more limited range of shot offsets, hence the reduced coverage compared to panel c.

While the 15t CO_2 plume was interpreted in Figure 6a was interpreted, it was not confidently above the detection threshold. The weak effects of the CO_2 saturation would not have been easily distinguished from the background residuals in an unexpected shallow leak scenario, without knowing where to look. In panels c and d of Figure 6, the 33 t CO2 plume has achieved sufficient saturation and extent in the BBRS reservoir to produce clear time-lapse anomalies above the level of the background residuals. These geophone results indicate that the plume's detection threshold was achieved between 15 t and 33 t of injection. The detection threshold is a product of both the CO_2 saturation and the lateral extent of the plume, which in this case is approximately 50 m for the 33 t injection amount. Inversion of the baseline and monitor data will be performed in the future, to better characterize the CO_2 saturations necessary to detect the CO_2 plume.

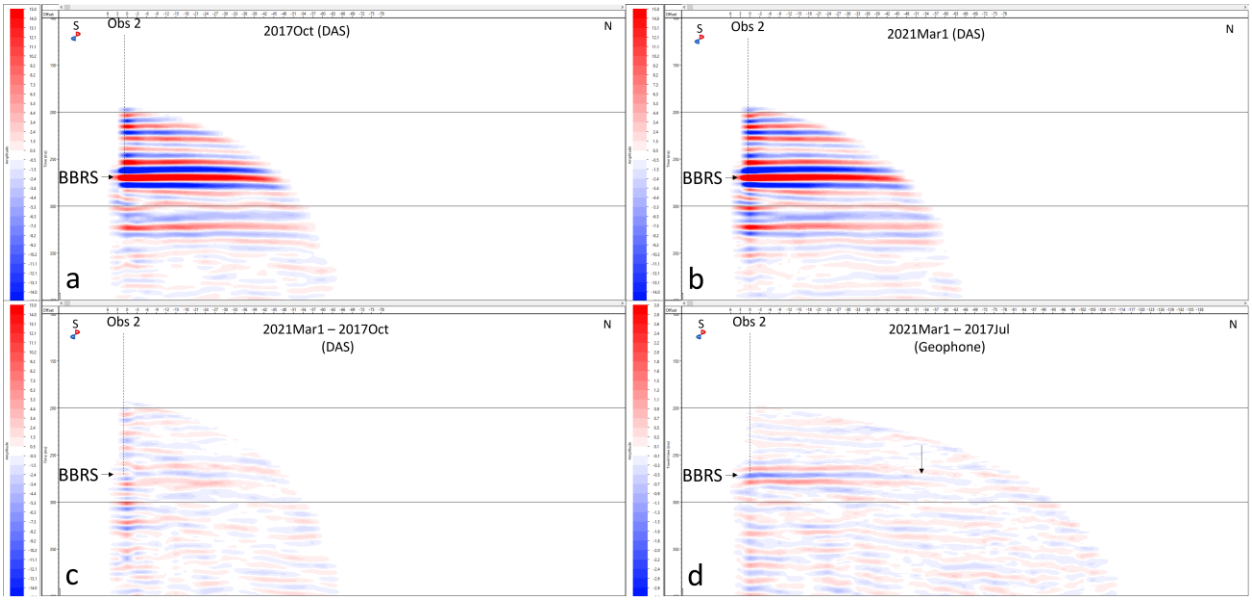

Figure 7. DAS baseline (a) and monitor (b) VSP CDP stacks and time-lapse difference (c). DAS trace depths were trimmed to 190m-305m for this display, equivalent to the geophone depths. The CO2 anomaly in the geophone data (d) is not as pronounced in the DAS data (c).

Although the 1-C time-lapse workflow could be directly applied to the straight-fiber DAS data available at CaMI.FRS, additional processing steps were required, such as: Spatial re-sampling, depth-registration, and aggressive de-noising of the raw DAS data (Kolkman-Quinn, 2022). The time-lapse result from the best quality DAS data is shown in Figure 7. The reduced lateral coverage is due to the DAS baseline data only extending to 150 m shot offset. Unlike the geophone data, the ambiguous DAS result is not clearly above the detection threshold. High noise levels in the raw data were found to cause sufficient dissimilarity between individual shot gathers to prevent the CO2 anomaly from clearly showing through the stack.

The successful detection of 33 t of CO_2 in the 300m deep sandstone reservoir of up to 10% porosity demonstrates the MMV capabilities and limitations of time-lapse VSPs. The challenges experienced with the DAS data indicate a larger CO_2 injection amount and correspondingly higher CO2 saturation will be needed to surpass the DAS detection threshold. These results were achieved with careful processing, and push the limit of detectability in this geological setting. The workflow and detection threshold should help inform MMV expectations for both shallow leak detection and shallow reservoir monitoring of CO_2 sequestration operations.

Acknowledgements

We would like to thank the sponsors of CREWES and CaMI for their continued support. This work was funded by CREWES industrial sponsors and NSERC (Natural Science and Engineering Research Council of Canada) through the grant CRDPJ 543578-19. The data were acquired through a collaboration with the Containment and Monitoring Institute (CaMI) of Carbon Management Canada (CMC). Research at the CaMI field site is supported by the Canada First Research Excellence Fund, through the Global Research Initiative at the University of Calgary.

References

Al Mutlaq, M., and Margrave, G., 2011, Short note: Shaping / Matching filters: *CREWES Research Report*, **23**, 2, 11.

Cheng, A., Huang, L., and Rutledge, K., 2010, Time-lapse VSP data processing for monitoring CO_2 injection: The Leading Edge, **29**, 196-199.

Dongas, J., 2016, Development and characterization of a geostatic model for monitoring shallow CO_2 injection: M.Sc. Thesis, University of Calgary.

Gordon, A., 2019, Processing of DAS and geophone VSP data from the CaMI Field Research Station: M.Sc. Thesis, University of Calgary.

Hinds, R.C., Anderson, N.L., and Kuzmiski, R.D., 1996, VSP Interpretive Processing: Theory and Practice: Society of Exploration Geophysics.

Macquet, M., Lawton, D., 2017, Reservoir simulations and feasibility study for seismic monitoring at CaMI.FRS: CREWES Research Report, **29**, 56.1-56.26.

Macquet, M., Lawton, D., Saeedfar, A., Osadetz, K., 2019, A feasibility study for detection thresholds of CO_2 at shallow depths at the CaMI Field Research Station, Newell County, Alberta, Canada: Petroleum Geoscience, **25**, 509-518.